



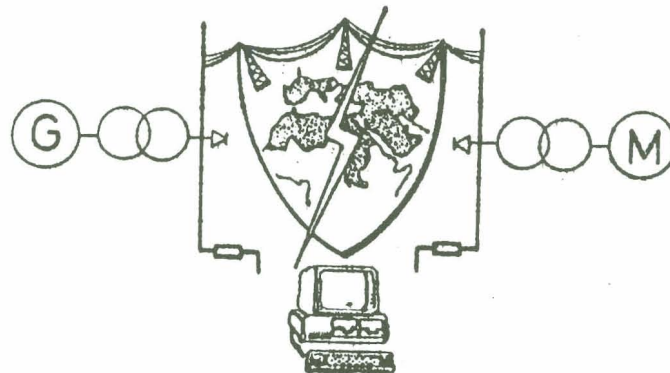
*Assiut University*

PROCEEDING OF THE  
SECOND  
**MIDDLE EAST POWER  
SYSTEM CONFERENCE**

**MEPCON'92**

**January 6-8 1992**

**Electrical Engineering Department  
Assiut University  
Assiut, EGYPT**



	Page
<b>Upgrading the Existing Egyptian 500 KV Transmission Network by Series Capacitor Compensation : Analysis of Transient Stability and SSR.</b>	
A. A. Shaltout, Jordan Univ. of Science & Tech., Irbid, Jordan, M. El-Marsafawy, Cairo Univ., Cairo, Egypt.	36
<b>Transient Studies of the Egyptian Unified Power System.</b>	
E. H. Shehab-Eldin, M. M. M. Mahmoud, Helwan Univ., Cairo, Egypt.	41
<b>static VAR System-Dynamic Behaviour Analysis.</b>	
T. S. Bhatti, D. P. Kothari, Indian Institute of Tech., new Delhi, India.	47
<b>Transient Stability Evaluation for Riyadh Electric System.</b>	
Z. El-Razaz, A. Al-Ohaly, King Saud Univ., Riyadh, Saudi Arabia, S. Al-Sohaibani, SCECO-Central, Riyadh, Saudi Arabia.	50
<b>Transient Stability Enhancement Using Phase Shift Transformer.</b>	
Part1: Effect of Phase Shift Transformer on Fault Clearing Time.	
Part2: Effect of Inserting a Phase Shift Transformer on the System after Clearing the Fault.	
Ahmed El-Gaafary, Minia Univ., minia, Egypt.	56
 <b>SESSION 3 : ELECTRICAL MACHINES</b>	
<b>A New Synchronous Motor for Mag-Lev Train With Integrated Lift &amp; Thrust Using a Trapezoidal Rail.</b>	
S. M. Al-Kasimi, Umm-El-Qura Univ., Saudi Arabia.	67
<b>Performance Improvement of Inverter Fed Linear Induction Motor.</b>	
I. Marongiu, Univ. Di Cagliari, Italy, A. Perfetto, Universita di Napoli, Napoli, Italy.	70
<b>A Generalized Mathematical Model of Variable Reluctance Motor.</b>	
I. Marongiu, M. Salis, Univ. Di Cagliari, Italy.	74
<b>Dynamic Performance of Permanent-Magnet and Conventional Synchronous Generators, A Comparison Study.</b>	
A. H. Morsi, El-Menoufia Univ., Shebin El-Khayma, Egypt.	80
<b>General Considerations on the Design of Switched Reluctance Motors.</b>	
A. Boglietti, M. Chiampi, D. Chiarabaglio, F. Profumo, M. Pastorelli, Politecnico di Torino, Torino, Italy.	85

## A NEW SYNCHRONOUS MOTOR FOR MAG-LEV TRAIN WITH INTEGRATED LIFT AND THRUST USING A TRAPIZOIDAL RAIL

S. M. Al-Kasimi

Assistant Prof., Elect. Eng. Dept., Umm-Ul-Qura University, Saudi Arabia.

Correspondance Address: P.O.Box 6112, Makka, Saudi Arabia.

Keywords: Zig-Zag, Trapezoidal, Linear, Homopolar, Synchronous, Machine, Maglev, Suspension, Propulsion & Transportation

### Abstract:

The paper describes an improvement to the Zig-Zag Linear Homopolar Synchronous Motor, ZZLHSM, providing a combined lift and thrust for maglev vehicles. A maglev vehicle is a vehicle that is supported by magnetic attraction between controlled dc electromagnets fixed to its chassis and a pair of iron tracks. The magnet of ZZLHSM is U-shaped and acts as a two-pole synchronous machine in which each pole is surrounded by dc coil feeding from a controlled dc power supply. Each pole is made up of two sub-poles surrounded by ac coil feeding from an inverter such that the field could be distorted among the four sub-poles. The rail of the ZZLHSM is zig-zag shaped and will move relative to the sub-poles to minimise reluctance, hence propulsion is obtained.

The improvement to the ZZLHSM described here is in the shape of the rail. A trapezoidal rail was chosen and the performance of the Trapezoidally Railed Linear Homopolar Synchronous Motor, TRLHSM, was compared to that of the ZZLHSM with same winding and excitation conditions. Theoretical analysis shows that two achievements were obtained:

1. One TRLHSM with a two-phase inverter drive can be used alone for self start propulsion, whereas two-phase pair ZZLHSM were required before.

2. Switching frequency in TRLHSM inverter drops to half that of ZZLHSM inverter for same motor speed.

### 1. Introduction:

Fig.1 shows the ZZLHSM magnet, in which the main poles are excited by dc coils with a net mmf of  $M_d$ . Each of the main poles is split into two sub-poles that are surrounded by ac coils. McLean<sup>[1,2]</sup> and West<sup>[1]</sup> have chosen a rail shape shown in Fig.2. Hence, with the ac coils around sub-poles excited such that the field is forced through sub-poles 1&3, the rail will move assuming constant air gap to link sub-poles 1&3. When field is forced through sub-poles 2&4, the rail will move again to link sub-poles 2&4. As the switching of sub-pole coil-excitations synchronizes to rail position, a continuous motion is obtained. The ZZLHSM is unable, due to symmetry, to start motion when the rail completely links sub-poles 1&3 or sub-poles 2&4 at a stop. Hence, to avoid this, another magnet is placed half pole-pitch away, where one pole-pitch,  $p$ , is the distance along axis of motion between starting edges of poles as shown in Fig.2. With two motors displaced  $p/2$  away, no symmetry position exists and the two-phase ZZLHSM motor pairs provide self start for one another.

Now for the same magnet, if a trapezoidally shaped rail like the one shown in Fig.3 is used, the ac coils around sub-poles can be excited to force field through sub-poles 1&3, and hence, the rail will move assuming constant air gap,  $Z$ , to link sub-poles 1&3. The field is then forced through sub-poles 2&3, hence, pulling the rail to link sub-poles 2&3. Forced through sub-poles 2&4, the field then pulls the rail to link sub-poles 2&4. Finally, when the field is forced into sub-poles 1&4, the rail will move to link them both. This completes one cycle and as excitations of sub-pole ac coils are synchronised to rail position, a continuous motion is obtained.

This Trapezoidally Railed Linear Homopolar Synchronous Motor, TRLHSM, is noted to have no symmetry position throughout its cycle. Hence, no need for a starter exists. Another feature is that the switching frequency is half that of the ZZLHSM for same speed, since the rail cycle length of the TRLHSM is twice that of the ZZLHSM.

### 2. Theoretical Analysis:

#### 2.1. Notations:

A sub-pole surface area

$e$  induced emf at ac coil terminals

F magnet thrust force

$\lambda_p$  peak flux linkage per ac coil

$\lambda_1$  flux linkage of ac coil around sub-pole 1

$\lambda_2$  flux linkage of ac coil around sub-pole 2

$\lambda_3$  flux linkage of ac coil around sub-pole 3

$\lambda_4$  flux linkage of ac coil around sub-pole 4

$M_d$  net dc mmf excitation of field winding

$M_a$  rms ac mmf excitation of armature winding

$N$  number of turns of ac coil around any sub-pole

$P$  ac input power

$p$  pole pitch

$T$  time period to complete one cycle

$t$  time

$u$  speed of rail relative to magnet

$\omega$  angular frequency of ac supply

$Z$  energised air gap

## 2.2. Assumptions:

The following assumptions were made in the analysis to come:

- All sub-poles have same surface area,  $A$ .
- AC colb around rub-poles are identical.
- Width of slot in the main poles is negligible.
- Fringing is negligible.
- Leakage is negligible.
- Steel loss is negligible.
- Copper loss is negligible.
- Air gap is homogeneous over the rub-pole#.
- Speed of motor relative to track is constant.
- Field mmf excitation,  $M_d$ , is constant.
- Flux linkage for each of the four ac coils varies sinusoidally between a maximum of  $\lambda_p$  ( when its sub-pole is fully coupled to the rail ) given by:

$$\lambda_p = \frac{N M_d A \mu_0}{2 Z} \quad (1)$$

and a minimum of zero ( when its rub-pole is fully uncoupled to rail ).

- Power factor seen by ac supply circuit is unity.

## 2.3. Review of Thrust Analysis of ZLHSM:

As the rail moves in the direction shown in Fig.2, flux linkages of ac coils will be obtained as shown in Fig.4, where  $\lambda_p$  is given in Eq.1. It is seen that these waveforms vary in-phase for the senses shown in Fig.2. Hence, to obtain maximum variation in flux linkage, the ac coils are connected as shown in Fig.5. Therefore, the total flux linkage at the terminal of the combined ac coils is given by:

$$\lambda = 2 \lambda_p \cos(\omega_Z t)$$

It is seen that these waveforms vary in-phase for the senses shown in Fig.2. Hence, to obtain maximum variation in flux linkage, the ac coils are connected as shown in Fig.5. Therefore, the total flux linkage at the terminal of the combined ac coils is given by:

$$\lambda = 2 \lambda_p \cos(\omega_Z t)$$

where the angular frequency of ZLHSM ac supply,

$$\omega_Z = \frac{2\pi}{T_Z}$$

with the duration to complete one ZLHSM cycle,

$$T_Z = \frac{2p}{u}$$

Hence:

$$\omega_Z = \frac{\pi u}{p} \quad (2)$$

Note that  $i = 0$  when sub-poles 1&3 are linked by rail. Hence, induced emf at combined ac coil terminals is given by:

$$e_Z = -2 \omega_Z \lambda_p \sin(\omega_Z t) \quad (3)$$

Hence, Input ac power,  $P_Z$ , for unity power factor, is given by:

$$P_Z = \frac{2 \omega_Z \lambda_p M_d}{4 \sqrt{2} N}$$

which, by using Eq.1, gives:

$$P_Z = \frac{M_d M_d A \mu_0 \omega_Z}{4 \sqrt{2} Z} \quad (4)$$

Thin electrical ac power,  $P_Z$ , is therefore directly converted into mechanical power via magnet thrust force,  $F_Z$ . Hence:

$$P_Z = F_Z u$$

Hence, using Eq.4:

$$F_Z = \frac{P_Z}{u} = \frac{M_d M_d A \mu_0 \omega_Z}{4 \sqrt{2} Z u} \quad (5)$$

and using Eq.2:

$$F_Z = \frac{\pi M_d M_d A \mu_0}{4 \sqrt{2} Z p} \quad (6)$$

Note that this is the force of one ZLHSM and that for self-start, two such motors are to be used in quadrature, both timewise in drives and displacementwise in their relative position to rail.

## 2.4. Thrust Analysis of TRLHSM:

On the other hand, when the rail of TRLHSM moves in the direction indicated in Fig.3, flux linkages of ac coils will assume linear segments and can be approximated to sinusoidal variation as shown in Fig.6, where  $\lambda_p$  is given in Eq.1.

It is seen that  $\lambda_1$  &  $\lambda_2$  vary in-phase with each other and that  $\lambda_3$  &  $\lambda_4$  also vary in-phase with each other but in quadrature with  $\lambda_1$  &  $\lambda_2$  coil variations. Hence, to obtain maximum variation in flux linkage per phase, the ac coils are connected as shown in Fig.7. Therefore, the total flux linkages at the terminals of the combined ac coils for both phases are given by:

$$\lambda_A = \lambda_1 + \lambda_2 = \lambda_p \cos(\omega_T t + 45^\circ)$$

$$\text{and: } \lambda_B = \lambda_3 + \lambda_4 = \lambda_p \cos(\omega_T t - 45^\circ)$$

where the angular frequency of TRLHSM ac supply,

$$\omega_T = \frac{2\pi}{T_T}$$

with the duration to complete one TRLHSM cycle,

$$T_T = \frac{4p}{u}$$

Hence:

$$\omega_T = \frac{\pi u}{2p} \quad (7)$$

Note that  $t = 0$  when sub-poles 1&3 are linked by rail. Hence, induced emf voltages at combined ac coil terminals for both phases are given by:

$$e_A = -\lambda_p \omega_T \sin(\omega_T t + 45^\circ) \quad (8)$$

and:

$$e_B = -\lambda_p \omega_T \sin(\omega_T t - 45^\circ) \quad (9)$$

Hence, input ac power,  $P_T$ , for unity power factor, is given by:

$$P_T = \frac{(m_A + m_B) \omega_T \lambda_p}{2\sqrt{2}N}$$

which, by using Eq.1, gives:

$$P_T = \frac{(m_A + m_B) M_d \lambda \mu_0 \omega_T}{4\sqrt{2}Z} \quad (10)$$

where:

$m_A$  is the rms ac mmf excitation of phase A armature winding, and  
 $m_B$  is the rms ac mmf excitation of phase B armature winding.

This electrical ac power,  $P_T$ , is therefore directly converted into mechanical power via magnet thrust force,  $F_T$ . Hence,

$$P_T = F_T u$$

Hence, using Eq.10:

$$F_T = \frac{P_T}{u} = \frac{(m_A + m_B) M_d \lambda \mu_0 \omega_T}{4\sqrt{2}Z u} \quad (11)$$

and using Eq.7:

$$F_T = \frac{\pi (m_A + m_B) M_d \lambda \mu_0}{8\sqrt{2}Z p} \quad (12)$$

Note that this is the force of one TRLHSM using a two-phase inverter drive for the ac colls, and that self start is guaranteed since no symmetry position occurs at any instant during one cycle.

### 2.5. Performance Comparison:

Firstly, as seen from Eqs.2&7, inverter frequency in TRLHSM is relaxed to half that of ZZLHSM for same speed  $u$ . Secondly, as seen from Eqs.3,8&9, induced EMF of TRLHSM per phase is quarter that of ZZLHSM. Thirdly, as seen from Eqs.4&10, in order to have same ac input power for both machines with same dc excitation,  $M_d$ , the ac mmf must be inversely proportional to the switching frequency. Hence, for the TRLHSM,  $(m_A + m_B)$  should be twice  $M_d$  for the ZZLHSM. This makes the expressions for the thrust forces, as seen in Eqs.6&12, identical and hence:

$$F_T = F_Z = \frac{\pi M_d M_d \lambda \mu_0}{4\sqrt{2}Z p}$$

### 3. Conclusion:

It is possible to achieve self start and to operate at a lower switching frequency when the shape of ZZLHSM rail is altered to trap-voidal one, keeping same excitation, inverter input power and speed.

### 4. Acknowledgment:

The author would like to express his thanks to Dr. S. Abu-Shadi at the electrical engineering department of King Abdul-Aziz University for his valuable assistance and comments.

### 5. References:

- [1] McLean, G. W. & West, A. N., "Combined Lift and Thrust for Maglev Vehicles Using the Zig-Zag Synchronous Motor", Proc. Int. Conf. on Maglev Transport Now and for the Future, IMechE, 1984, pp. 87-97.
- [2] McLean, G. W., "Review of Recent Progress in Linear Motors", IEE Proc., Vol. 35, Part B, No. 6, Nov. 1988, pp. 380-416.

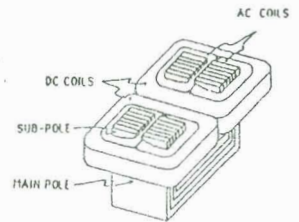


FIG. 1 ZZLHSM MAGNET SHOWING LAMINATIONS

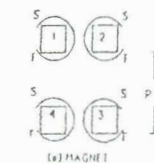


FIG. 2 (a) MAGNET & (b) RAIL OF ZZLHSM (CYCLE LENGTH = 2P)

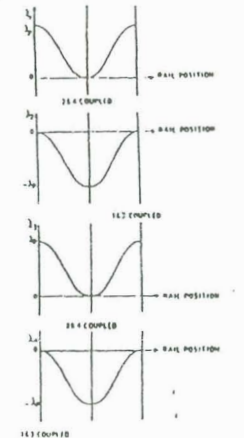


FIG. 4 FLUX LINKAGES OF AC COILS IN ZZLHSM VS RAIL POSITION

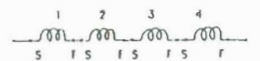


FIG. 5 COMBINED CONNECTION OF AC COILS IN ZZLHSM

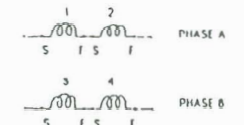


FIG. 6 PHASE CONNECTIONS OF AC COILS IN TRLHSM

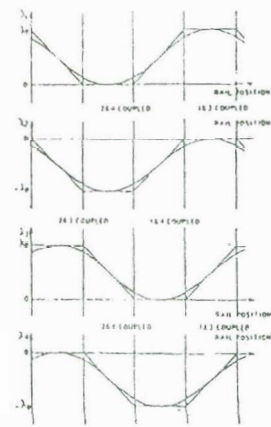


FIG. 7 FLUX LINKAGES OF AC COILS IN TRLHSM VS RAIL POSITION